


S. NAUMOV
E. SOROKIN
V.L. KALASHNIKOV
G. TEMPEA
I.T. SOROKINA 

Self-starting five optical cycle pulse generation in Cr⁴⁺:YAG laser

Institut für Photonik, TU Wien, Gusshausstr. 27/387, 1040 Vienna, Austria

Received: 2 May 2002/Revised version: 16 July 2002
Published online: 8 January 2003 • © Springer-Verlag 2003

ABSTRACT We report stable self-starting near-transform-limited 26-fs pulses at 250-mW output power from a Kerr-lens mode-locked (KLM) Cr⁴⁺:YAG laser using chirped mirrors in combination with prisms. The highest output power achieved in KLM regime was 600 mW at 55-fs pulse duration. The experimental results agree well with the results of theoretical analysis with respect to KLM self-starting ability and stability against continuous-wave and multi-pulse operation. Parameter ranges for stable transform-limited KLM pulses as well as the shortest achievable pulse durations are established. Using an InGaAs-InP semiconductor saturable absorber mirror we could obtain self-starting 57-fs pulses at the average output power of 200 mW. Two-photon absorption was found to be the main mechanism favoring the multiple-pulse operation.

PACS 42.70.Hj; 42.55.Rz

1 Introduction

Cr⁴⁺-doped YAG crystals [1, 2] have attracted a lot of attention of researchers since the late 1980s due to their capability to operate in the wavelength range around 1.5 μm , which is very interesting for many applications, and produce broadly tunable ultra-short pulses [3–5]. Among the fundamental advantages of Cr:YAG lasers are robustness, good thermal properties, the high small-signal figure of merit [6], defined as the ratio of attenuation at the maximum of absorption to attenuation at the lasing wavelength, suitability for direct diode pumping with InGaP/GaAs/InGaAs laser diodes [7, 8], and finally, the broad amplification bandwidth, offering a wide tuning range between 1.34 and 1.6 μm [2] and extremely short pulse durations at high peak powers [9–12]. The broad absorption band of Cr⁴⁺:YAG is centered around 1 μm and makes this material attractive for pumping with diode lasers [7, 8] as well as with high-power diffraction-limited sources based on diode-pumped Nd:YAG, Nd:YVO₄ [13–15], or Yb-fiber lasers [16]. Compact mode-locked sources of tunable femtosecond pulses are especially interesting for testing fibers in telecommunications, dense wavelength division

multiplexing technique, for optical coherence tomography in medicine, and for remote sensing and trace-gas monitoring via overtone molecular analysis.

1.1 Background results

Passive mode locking of Cr⁴⁺:YAG has been achieved using various techniques such as Kerr-lens mode locking (KLM) [9–13, 15, 17–19], regeneratively initiated mode locking [10], synchronous pumping [12], as well as using a semiconductor saturable absorber (SESAM) [14, 20–24]. The KLM scheme allowed generation of pulses as short as 43 fs at 200 mW of average power [15], a result that has remained unsurpassed for some years. The pulse duration was limited by the high third-order dispersion (TOD), which amounted to $\sim 9000 \text{ fs}^3$ [15]. We should note that especially in the case of the prism-dispersion-compensated Cr:YAG laser the TOD is significant and practically unavoidable. Although they have some asymmetry, introduced by TOD to the pulse spectra [28, 29] and the increased side-band generation [30, 31], these pulses were near-transform-limited and self-starting [17]. Very recently, the 40-fs barrier has been overcome and a pulse duration of 20 fs has been demonstrated [32], using only double-chirped mirrors for dispersion compensation [33]. The maximum output power reached 400 mW in these experiments. The SESAM-based devices allow developing practical self-starting sources of ultra-short pulses. The shortest pulses obtained so far in Cr⁴⁺:YAG using the broad-band gold-reflector-based SESAM are 44 fs at 65 mW at 1520 nm [22, 23]. High-repetition-rate (up to 2.7 GHz) femtosecond Cr⁴⁺:YAG lasers have also been demonstrated [24–27] using both techniques.

1.2 Aims and outline

The present work is aimed at the development and investigation of possibilities of the compact self-starting Cr:YAG laser source, generating only few optical cycle pulses. Both approaches to self-starting – a pure KLM as well as a SESAM-assisted self-starting – were successfully implemented. The investigation included experimental as well as numerical studies of the parameter limits of the system in terms of self-starting, stability, achievable output power levels, and pulse durations at good pulse quality. The latter implies a possibly chirp-free pulse envelope with a smooth

 Fax: +43-1/58801-38799, E-mail: sorokina@tuwien.ac.at

spectrum, the maximal pulse energy, and the minimal CW contribution.

In this paper we report what is to our knowledge the first self-starting KLM Yb-fiber laser pumped Cr⁴⁺:YAG laser, generating highly stable near-transform-limited pulses at down to 26-fs pulse duration at 250–450-mW output power. The maximum average output power of 55-fs pulses was 600 mW, which is the highest reported mode-locked output power for a Cr⁴⁺:YAG laser so far.

As an alternative, we also realized a self-starting regime using a SESAM, where 57-fs pulses at 200-mW output power and ~ 70 -fs pulses at 230-mW output power could be routinely obtained. This output power level compares with the results reported in [22, 23] (180 mW, ~ 60 fs) and is noticeably higher than that of the lasers with the semiconductor Bragg-mirror SESAMs (40–90 mW, ~ 110 fs [14, 20, 21]).

Finally, we present the results of the theoretical analysis of our laser with respect to KLM self-starting ability and stability against CW and multi-pulse operation. The analysis is based on numerical simulations using the real experimental parameters and provides the insight on the theoretically achievable pulse durations and the spectral position of the pulse within the gain curve and defines stability limits for transform-limited pulses. The results of numerical optimization are in good agreement with experimental results.

2 Experimental setup

The experimental setup is shown in Fig. 1. As a pump source we used a 30-W CW polarized single transversal mode diode-pumped Yb-fiber laser (IPG Laser GmbH) operating at 1070 nm. To control the overlap of the pump mode with the resonator mode we used a telescope consisting of 75-mm and 70-mm lenses. The total throughput of the focusing system was 93%. One of the lenses was mounted on a translation stage, so that by varying the distance between the two lenses one could change the pump spot size inside the active medium. Using the knife-edge technique we measured the pump spot size in the laser crystal. The optimum pump spot size was adjusted each time experimentally and varied between 110×200 and $130 \times 235 \mu\text{m}^2$.

2.1 Resonators for KLM experiments

For the initial KLM mode-locking experiments we used an astigmatically compensated X-fold four-mirror cavity design as shown in Fig. 1a. A 20-mm-long, 5-mm diameter, Brewster-cut Cr⁴⁺:YAG crystal was mounted on a water-cooled brass block and kept at $\sim 12^\circ\text{C}$. The crystal had a small-signal absorption of 1.1 cm^{-1} at the pump wavelength, and passive losses of $\sim 1.7\%$ per pass. At typical pumping levels the real absorption was less due to the saturation. The real absorbed power, which is referred to throughout the paper, was therefore measured directly. The cavity consisted of the two concave mirrors, M1 and M2, with 100-mm radius of curvature, the high-reflective (HR) end mirror M3, and the output coupler (OC). The pump light was focused through the dichroic concave resonator mirror M2 by a 10 cm focal length lens. The HR mirrors were centered at 1500 nm and were ~ 350 -nm broad. Each HR mirror had losses less

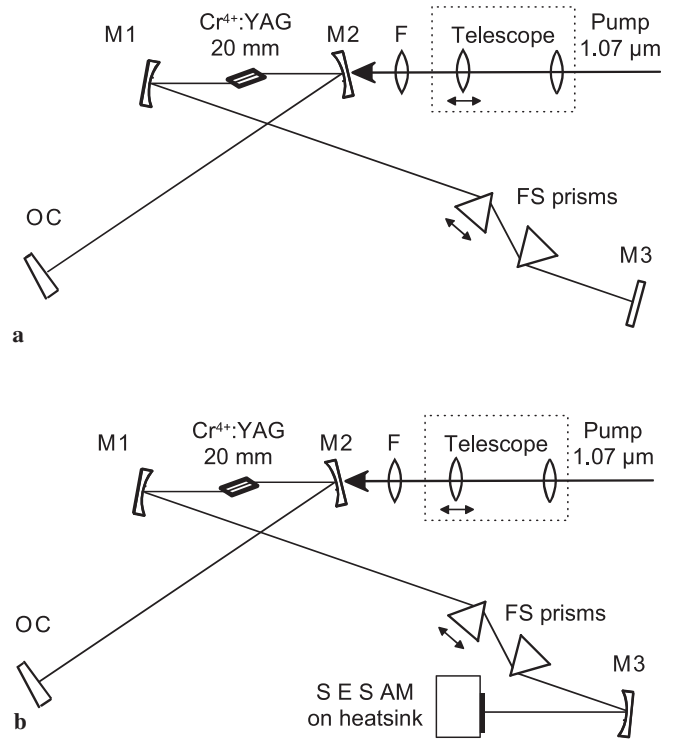


FIGURE 1 Scheme of KLM X-cavity Cr⁴⁺:YAG laser design (a). Mirrors M1 and M2 are 100-mm radius of curvature (ROC). M1 is a chirped mirror, M2 and M3 are standard dielectric mirrors and OC is the output coupler with transmission 0.5%–1.5%. Mode locking with SESAM (b). Mirror M3 is replaced by the concave focusing mirror with ROC 50–200 mm and a SESAM on a heat sink

than 0.05% at the laser wavelength and transmitted approximately 95% at the pump wavelength. The total cavity losses (excluding those due to the output coupler) were measured to be $\sim 4\%$. The OC transmission varied between 0.5% and 1.5% of the nominal transmission (OC spectra can be seen in Fig. 7a).

In the course of the experiment, in order to reduce the pulse-repetition rate and to increase the pulse energy, we increased one of the resonator arm lengths up to 2 m. In order to keep the resonator mode waist the same as in the shorter resonator the chirped mirror M1 was exchanged by a high reflector with 150-mm radius of curvature. In order to preserve the net cavity group-delay dispersion (GDD) we inserted a chirped folding mirror M3.

2.2 Dispersion-compensation schemes

For dispersion compensation we used both dispersive ‘chirped’ mirrors (CMs) and a conventional pair of fused-silica prisms in order to provide the possibility of fine tuning of the dispersion on the one hand, and reduce the effect of the oscillations of the GDD on the other hand. These residual oscillations are practically unavoidable for CMs [33]. Invented in 1994 [34], dispersive CMs are multi-layer dielectric stacks capable of providing high reflectance and accurate control of the group delay and higher-order dispersion over extended bandwidth. Initially, CMs were designed by means of computer optimization [34] and had limited bandwidth (e.g. ~ 200 nm at 800 nm). With the advent of quasi-

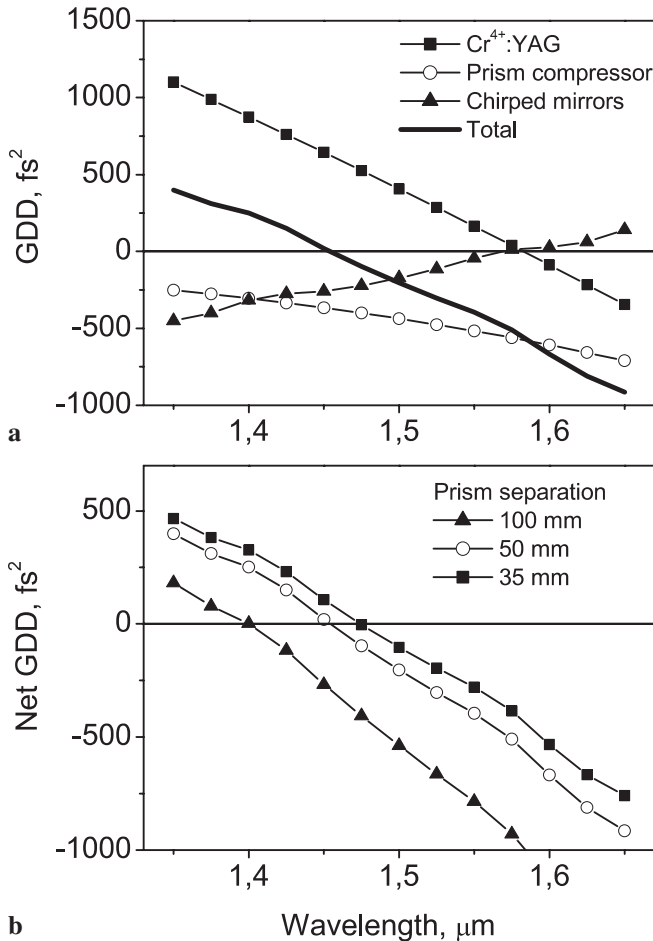


FIGURE 2 Dispersion characteristics of the intracavity elements (a): the Cr:YAG crystal, the prism pair (apex distance 50 mm), and the chirped mirrors (two bounces). Calculated round-trip cavity dispersion (b). *Open dots* for prism separation 50 mm (optimum), *solid dots* for prism separation 35 mm. Decrease of the prism dispersion causes the pulse spectrum to shift to red wavelengths in order to remain within negative dispersion values

analytical pre-design methods [35, 36], the properties of CMs could be largely enhanced: the bandwidth could be extended up to 160 THz (more than 300 nm) and dispersion could be engineered up to the fourth order. Using the design method described in [36], a CM design tailored for a Cr:YAG oscillator was realized. To reduce scatter loss the mirrors were evaporated using the ion-beam-sputtering technique. The mirrors were designed to have a negative second-order dispersion of approximately -80 fs^2 per bounce at 1500 nm. The calculated GDD of the mirror is given in Fig. 2a. The CM compensates the cavity dispersion up to the third order and provides high reflectance ($> 99.9\%$) in the wavelength range 1320–1670 nm. For comparison the GDD of a Cr:YAG crystal and the prism pair is given in the same figure separately.

2.3 Setup using a SESAM

Alternatively to KLM, we have also implemented an InGaAs/InP semiconductor saturable absorber mirror [37] as a starting mechanism for passive mode-locking operation. The SESAM consists of a 6-nm InGaAs quantum well (absorbing around $1.5 \mu\text{m}$) sandwiched between $\lambda/4$ and λ layers

of InP. The structure has a broadband HR coating on the rear side, and an anti-reflection coating on the front side. Two different SESAMs were available for experiments. The low-absorbing sample had an excitonic absorption maximum around 1450 nm and provided initial absorption of $\sim 2\%$. The high-absorbing sample had the double-peak excitonic band with maxima around 1450 and 1500 nm, respectively, and initial absorption of 3.5% at 1500 nm. The cavity design is shown in Fig. 1b with the HR mirror M3 replaced by a concave focusing mirror and a SESAM, attached to the aluminum heat sink at room temperature.

3 Results and discussion

Self-starting mode-locking operation of the system was one of the primary goals of this work. Self-starting can build up from spontaneous fluctuations in a KLM scheme or can be ensured by using a SESAM as a starting mechanism. We have investigated both these approaches. Initiation of the KLM without a saturable absorber usually requires some external perturbation such as, for example, tapping on one of the mirrors. However, it is possible to achieve self-starting in a symmetrical laser cavity [38] although cavity adjustment becomes quite critical. The use of a SESAM conveniently provides mode-locking operation, but relatively high insertion losses of a SESAM reduce the average output power of the mode-locked laser.

3.1 CW operation

The laser has been first optimized in CW operation, where it demonstrated an output power of up to 2.1 W at 20 W of incident power. The OC transmission was 1.5% and the threshold pump power 2 W. The arm lengths were set to 45–50 cm, providing a waist diameter in the crystal of $\sim 80 \mu\text{m}$ (in the saggital plane), close to the pump waist diameter of $\sim 100 \mu\text{m}$. Increasing the pump power resulted in a decrease of the output power, caused by the thermal run-off. With the birefringent quartz plate the laser wavelength could be tuned over 300 nm (from 1335 to 1635 nm) in the case when all mirrors were high reflectors and over 220 nm (from 1355 to 1575 nm) with a 1.5% output coupler.

3.2 Kerr-lens mode locking

Efficient KLM action could be obtained with the symmetrical resonator, when the arm lengths were increased to 70 cm and made equal within 1-cm accuracy [38]. In CW operation this resonator yielded more than 1 W of output power for approximately 7 W of absorbed pump power (9.2-W incident power), limited by thermal effects. The resonator mode waist size for efficient soft-aperture KLM [39] was optimized experimentally and was calculated to be $\sim 60 \times 110 \mu\text{m}^2$, i.e. noticeably less than the pump spot size, thus explaining the efficiency decrease. In the mode-locked regime the laser yielded up to 450 mW of output power through a 1.5% output coupler with the pulse duration $\sim 35 \text{ fs}$. Increasing the intracavity power by reducing the output-mirror transmission to 0.5%, we obtained pulses as short as 26 fs at 250 mW of output power for 6 W of absorbed pump power (Fig. 3a,b). The experimental autocorrelation trace is

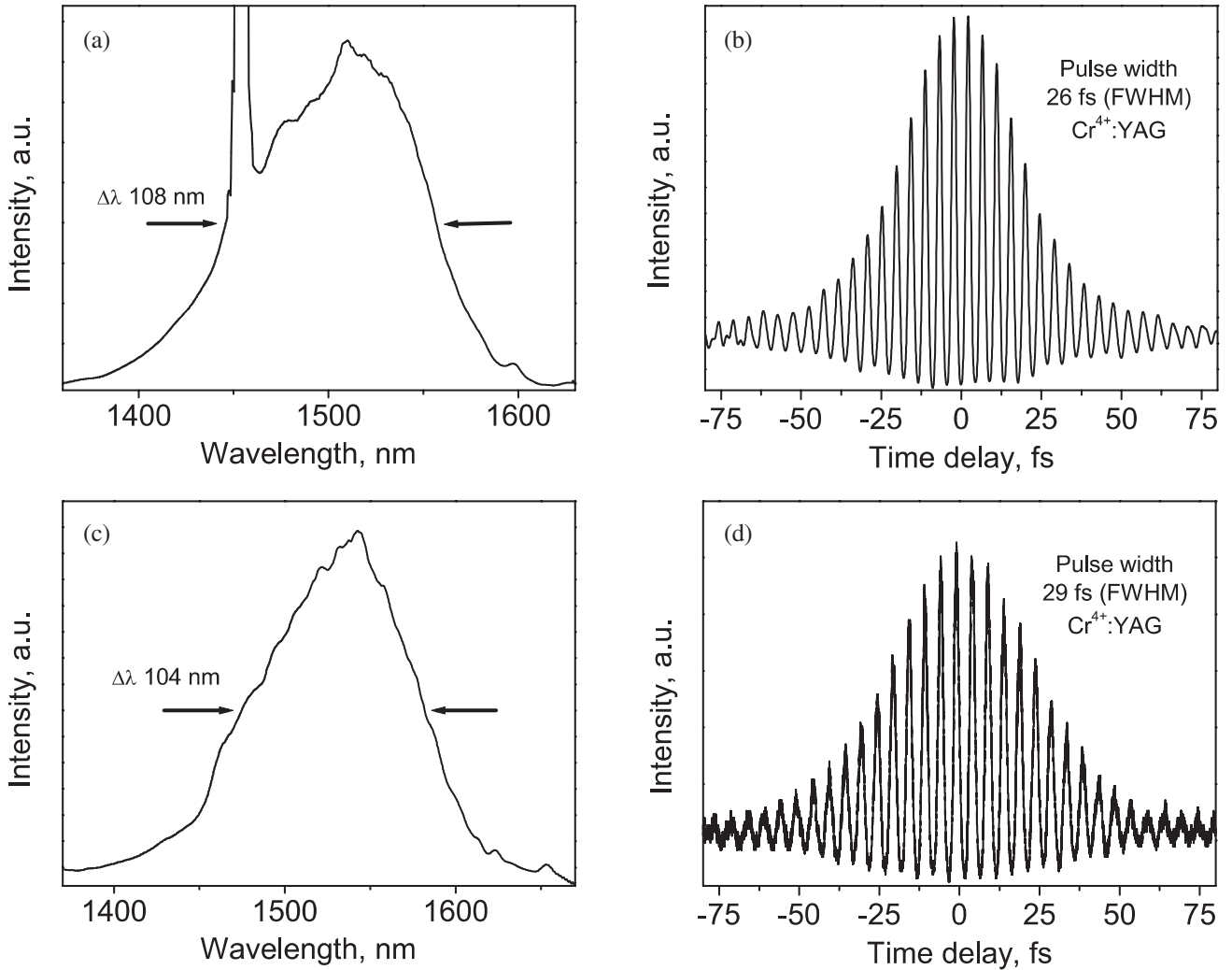


FIGURE 3 Spectrum (a) and interferometric autocorrelation (b) of a 26-fs pulse. Absorbed pump power 6 W, output power 250 mW, including the CW component at 1450 nm. Spectrum (c) and interferometric autocorrelation (d) of a 29-fs pulse, at 5.5 W of absorbed pump power and 60 mW of output power

well fitted with the calculated fringe-resolved autocorrelation trace, with close to the sech^2 pulse shape. The time-bandwidth product of 0.34 indicates that generated pulses are near-transform-limited. The mode locking was self-starting, easily reproducible, and remained stable for hours. The CW component at 1450 nm was caused by the excess energy inside the resonator, and could be reduced by lowering the pump power, to obtain a clean spectrum at lower output power and somewhat longer pulse duration of 29 fs (Fig. 3c,d). The reason for this behavior is described in more detail in conjunction with Fig. 7 (see below).

It is worth mentioning that purging of the resonator with dry nitrogen led neither to shorter pulses nor to any significant improvement in the mode-locking stability. Therefore, all the results described in this paper were obtained without the purging of the cavity.

The chirped mirrors were designed to have negative second-order and negative third-order dispersion to compensate for positive dispersion of the laser material. After taking into account the two bounces on the chirped mirror and dispersion of the laser crystal and prisms we estimate the net GDD per round trip to be zero at 1.45 μm and -400 fs^2 at 1.55 μm

(Fig. 2b). By varying the prism separation we could finely control the second-order dispersion (Fig. 2b).

Figure 4a shows the dependence of the pulse spectrum width (FWHM) on the prism apex-to-apex separation. One can see that the optimum separation is 50 mm, corresponding to the spectrum width of more than 100 nm, and the corresponding pulse duration is ~ 26 fs. According to the theoretical predictions, described in Sect. 4, the Kerr-lens modulation depth had to be increased in order to maintain stable KLM operation while reducing the prism separation beyond the optimum value. In a soft-aperture KLM scheme, this could be achieved by changing the pump beam focusing and cavity readjustment. The shortest distance between prisms, at which stable mode locking was still achievable, was 35 mm. Interestingly, reduction of the net GDD did not lead to further pulse shortening as expected. The spectral bandwidth of the pulse drastically decreases during the attempt to further reduce the net GDD below the optimum value. This may be due to the shift of the negative-GDD region further into the infrared with decreasing prism separation, as illustrated in Fig. 2b. Although within the soliton theory the TOD in the first order cannot lead to significant pulse spectral shifts [40]; in

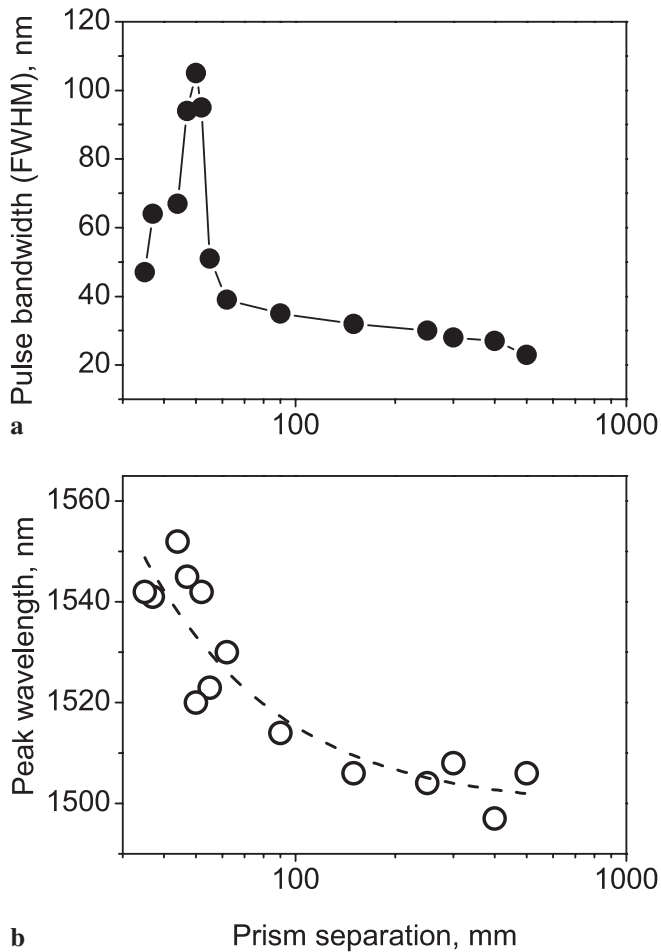


FIGURE 4 Pulse spectrum width (a) and central wavelength (b) dependence on prism separation. X axis is shown on logarithmic scale. 25-nm spectrum corresponds to 150 fs pulses and 105 nm spectrum to 25 fs pulses. Prism separation is measured from apex to apex

our case we deal with the indirect effect of the TOD. As will be shown in Sect. 4, there always exists a certain minimum negative net GDD, allowing for stable KLM. Therefore, the contribution of the high-order dispersion may effectively shift this minimum net GDD, thus changing the spectral position of the pulse [41] (compare Figs. 2b and 4b). For the same reason, in the presence of the fourth-order dispersion, the pulse spectrum follows the dip in the cavity dispersion curve. This effect can be especially clearly observed in Gires–Tournois interferometer mirror dispersion controlled resonators [42].

However, although the above explanation is straightforward, there may be still several other mechanisms of the pulse shift [41], the induced Raman scattering being one of them [40, 43]. At the same time, we could exclude the explanation of the shift that is common in the literature, as being due to the water absorption in the resonator, since purging the cavity with dry nitrogen did not produce any noticeable change either in the pulse duration or in its spectral position. Besides, the longer picosecond pulses are always generated in our cavity at the maximum of the Cr:YAG gain ($\sim 1.45 \mu\text{m}$).

In order to increase the pulse energy we reduced the pulse-repetition rate from 100 MHz to ~ 65 MHz by increasing the resonator length as described in Sect. 2.1. However, the in-

creased pulse energy did not lead to pulse shortening. This may be due either to the remaining uncompensated third-order dispersion or to the limiting effect of the output-mirror transmission at the red side.

Figure 5 summarizes the output characteristics in CW and mode-locked regimes. To achieve the maximum output power we adjusted the spot size of the pump beam for the optimal overlap with the resonator mode. In this way pulses as short as 55 fs at 600-mW output power have been produced (open dots in Fig. 5). This is to our knowledge the highest reported average output power in the mode-locked Cr⁴⁺:YAG laser so far. The pulse energy was 9.4 nJ, corresponding to the peak power of 170 kW. In CW regime the laser yielded 760 mW of output power. A tighter focusing of the pump beam allows for stronger mode discrimination, making pulses more stable but, as was mentioned above, in the case of Cr:YAG it reduces the output power. A compromise solution lies between the two poles: increased mode-locking stability at the cost of the somewhat reduced average power (solid dots in Fig. 5). One can notice that thermal loading limits the output power of the laser for absorbed pump powers above 6 W. When the laser was optimized for a lower KLM threshold, stable pulses could be achieved at an absorbed pump power down to 3 W (this corresponds to 4.8 W of the incident pump power).

By increasing the pump power within the stable mode-locking range we were able to shorten the pulse duration from 33 fs at 5 W of absorbed pump power to 26 fs at 6 W of absorbed pump power without compromising the pulse stability. The corresponding pulse spectrum broadened from 71 nm to 113 nm (Fig. 6). The spectrum broadening occurs mainly on the blue side, because on the red side the spectrum is limited by the transmission of the output coupler. In the pulse spectrum one can notice a CW component. Noticeably, but similarly to Tong et al. [17], the self-starting of our laser was also always accompanied by a CW component in the spectrum. Without the CW component the laser required tapping on the mirror for starting of mode locking. In Fig. 7 the pulse spectra taken using the 1.5% and 0.5% output couplers are compared for two cases: outside the resonator (Fig. 7a) and

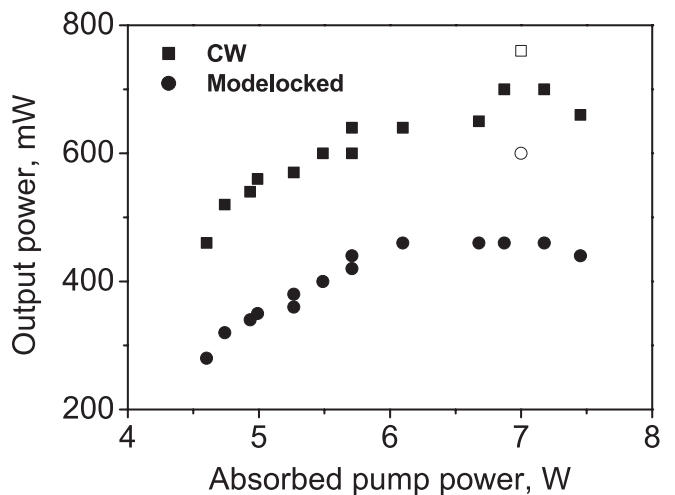


FIGURE 5 Output characteristics in CW (squares) and mode-locked (circles) regimes. Open dots correspond to best pump and resonator mode overlapping. Solid dots were with mode-overlapping optimized for KLM stability

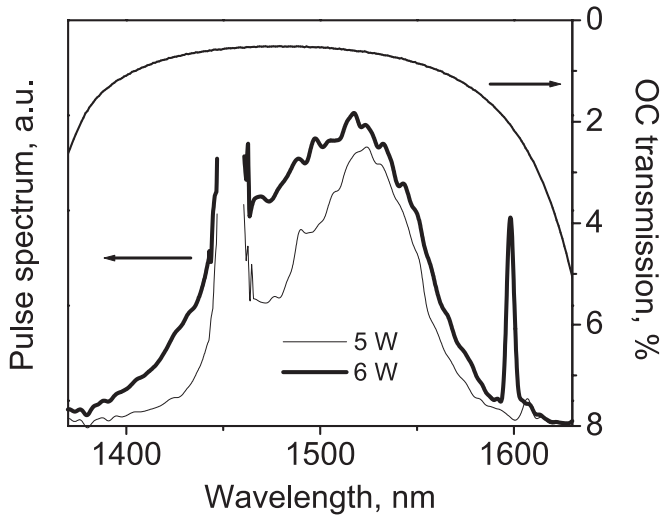


FIGURE 6 Pulse spectra for various pump powers (*left-hand axis*). *Thick line* corresponds to 6 W of absorbed pump power and *thin line* to 5 W. Output-mirror transmission (*right-hand axis*) limits pulse broadening

inside the cavity (Fig. 7b). Since all the other parameters except for the output transmission were kept the same, we could expect that a higher intracavity pulse energy would lead to broadening of the intracavity pulse spectrum. On the contrary, no change in the spectral shape inside the resonator could be observed (Fig. 7b). The laser obviously shed all the excess energy into the CW component, which served as a reservoir for the remaining energy. To understand that, we recall that the self-starting regime requires a very high self-amplitude-modulation (SAM) coefficient at low intensity. This leads to

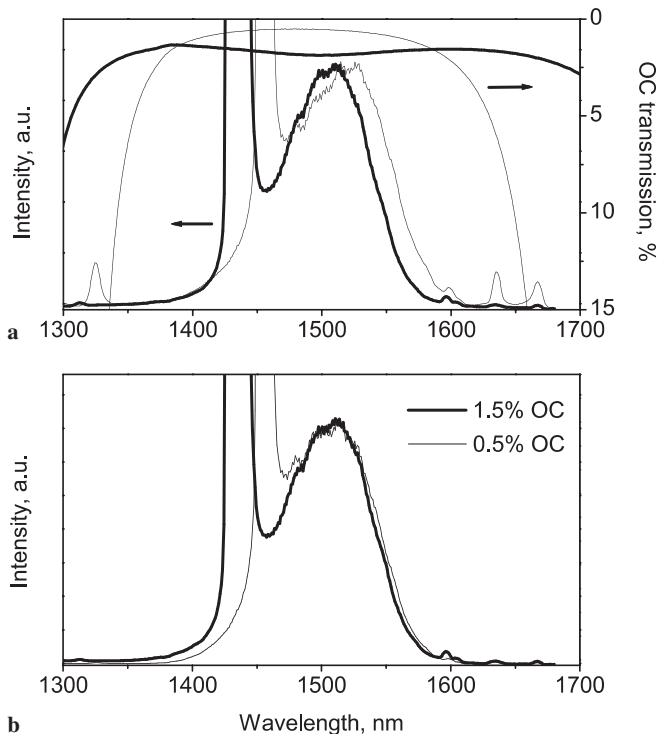


FIGURE 7 Pulse spectra with different output couplers. Output spectra together with OC transmission curves (a). Spectra inside the cavity (b). On both plots *thick line* corresponds to the 1.5% OC, *thin line* to the 0.5% OC

easy saturation of the SAM at high intensities, corresponding to the ultra-short pulse, thus allowing the CW component to coexist alongside with the pulse. This operation regime has been theoretically described [44], where it was predicted that an increase of the pumping rate over a certain value should cause CW component growth at constant pulse energy (see Fig. 4c in [44]). This description fits very well to what we have reproducibly observed in the experiment (Fig. 7; also compare Fig. 3b,d).

Another result of the saturation of the SAM at excess pulse energy may be the pulse break-up. We have repeatedly observed the multiple-pulse mode-locking regime, when there are two or more pulses in the resonator per round trip. At a low pump rate there is a single pulse per round trip, but with increasing pump power the pulse would split into two, three, or more pulses (Fig. 8). It is interesting to note that, within experimental error, the multiple pulses have equal energies, but in the case of three or more pulses the time delays between pulses are not equal (Fig. 8d). At the same time, the pulses maintain fixed time delays and phase relations with respect to each other for tens of seconds, evidenced by the stable interferometric autocorrelation signal and spectrum, respectively (Fig. 8).

We can conclude, therefore, that the self-starting KLM regime, although convenient for applications, is prone to instabilities against the CW component and multiple-pulse operation, except for the relatively narrow range of pump rates above the mode-locking threshold.

3.3 SESAM mode locking

As an alternative to self-starting KLM we have also investigated a SESAM-initiated mode locking. In the setup of Fig. 1b, several focusing mirrors between 50- and 200-mm radius of curvature were tried in order to optimize the spot size on the SESAM. The best results were obtained with mirrors of 100- and 150-mm radii of curvature.

Self-starting mode locking could be achieved with both SESAMs. The low-absorbing SESAM was prone to Q-switched operation, which could be avoided at higher pump power and smaller spot size. With optimized dispersion and the spot size on the SESAM of $\sim 100\text{-}\mu\text{m}$ diameter, the laser could provide up to 230 mW of average output power with pulses of about 100-fs duration. Such short pulses, however, could be obtained only in the multi-pulse regime, with a pulse train of up to 10–30-ps duration, with three or more pulses in the train.

The high-absorbing SESAM behaved quite differently. Due to the high initial absorption, the oscillation threshold was significantly higher than with the HR mirror. At the same time, when started, the laser always operated in the mode-locked regime, without Q-switching at any pump power and spot size. With this SESAM, the laser delivered pulses as short as 57 fs at 200 mW of average output power (Fig. 9a). Further increase of the output power to 230 mW was accompanied by the increase of the pulse duration to 70 fs. Mode locking occurred in a wide range of pump powers (between 3.5 and 13 W of the incident power), even close to the laser threshold (1.8 W absorbed power, corresponding to 3.5 W of incident power), although in the latter case the pulse dura-

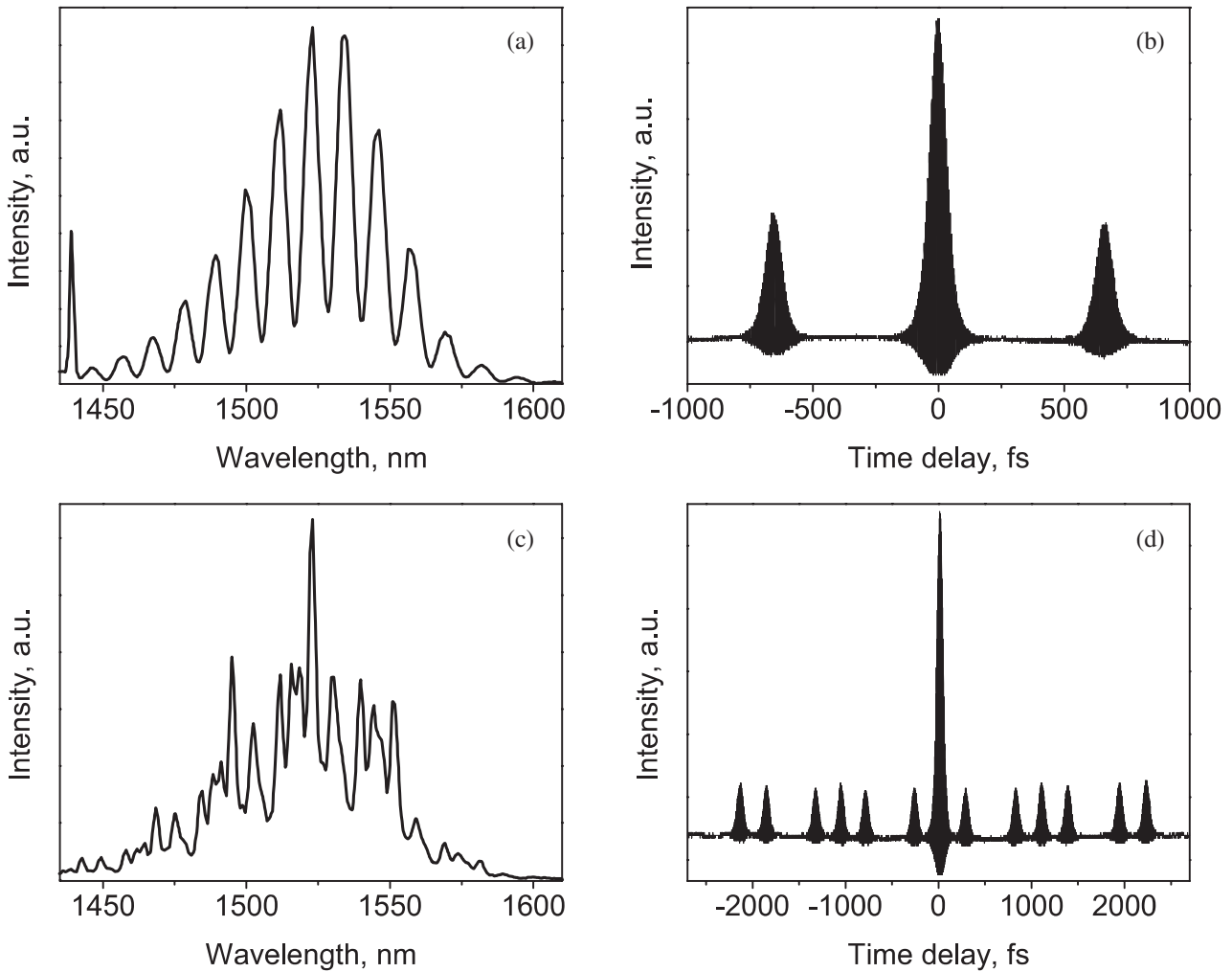


FIGURE 8 Generation of multiple pulses. Spectrum (a) and autocorrelation (b) of double pulses. Absorbed pump power 6.4 W. Spectrum modulation depth and frequency depend on delay between the pulses. Spectrum (c) and autocorrelation (d) of four pulses. Absorbed pump power 7.2 W. In this case pulses are separated unequally

tion increased significantly. The laser typically demonstrated hysteresis behavior: after oscillation started, the pump power could be reduced to 50%–70% of its threshold value without interrupting the operation. With this SESAM, as with the low-absorbing one, the ultra-short-pulse oscillation was typically observed in the multiple-pulse regime. The single-pulse regime could only be guaranteed with longer (up to picosecond-duration) pulses, obtained with large intracavity dispersion. At low pump power, the laser operates at 1460 nm, corresponding to the short-wavelength maximum of the excitonic band. By increasing the absorbed pump power we observe the shift of the pulse spectrum towards the second maximum of absorption of the SESAM structure at 1.5 μm (Fig. 9b). The pulse cleans up from the continuum and the periodic modulation due to multi-pulsing becomes more visible.

The tendency to multiple-pulse operation has been observed before in the SESAM-mode-locked Cr:YAG lasers [20, 24] and attributed to the saturation of the SAM when the instantaneous intensity of the pulse becomes too high as a result of the pulse shortening. In a separate study, two-photon absorption (TPA) was found to play a significant role at inten-

sities about 1–10 GW/cm^2 in similar SESAM structures [45]. At moderate intensities the TPA can play a stabilizing role against Q-switching instability, but at high intensities the effect of the TPA is to limit the pulse-intensity growth, i.e. provoking the pulse break-up. In our laser, the intensity of a single 100-fs pulse having the energy fluence of up to 4 mJ/cm^2 exceeds the above value by an order of magnitude and would have experienced prohibitively high losses. For a given SESAM design, however, the ratio of the SAM-incurred gain to the TPA-induced loss cannot be changed by cavity design or dispersion optimization. As the peak pulse intensity inversely scales with the pulse width (if a soliton-like pulse-shortening mechanism prevails, the peak pulse intensity scales as an inverse square of the pulse width), the TPA-induced pulse break-up may become a major obstacle to pulse shortening.

The largest contribution to the TPA comes from the surrounding InP layers, with the overall thickness of 590 nm [37]. On the contrary, the absorbing InGaAs layer has a thickness of about 6 nm, thus providing a negligible contribution to the TPA. This enables a certain design freedom, making it possible to reduce the TPA contribution by growing thinner

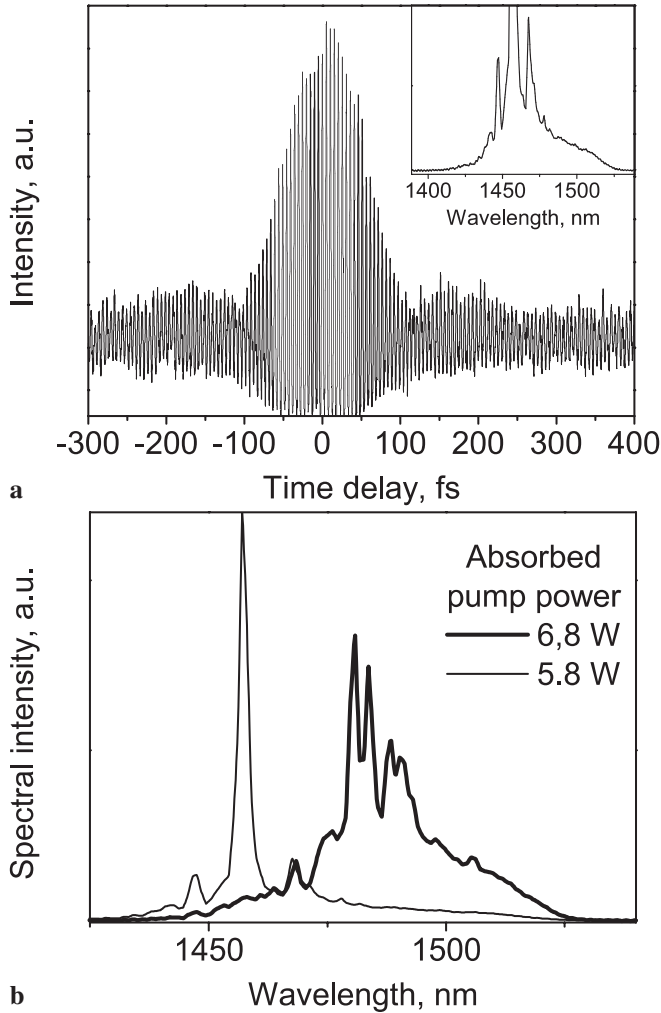


FIGURE 9 Intensity autocorrelation trace and pulse spectrum (*inset*) of mode-locked laser with SESAM (a). Pulse duration 57 fs assuming a Gaussian pulse shape. Pulse spectrum shift for different absorbed pump powers (b). Waist radius on SESAM $\sim 50 \mu\text{m}$.

surrounding InP layers, or by substituting InP with a material having a lower TPA coefficient, e.g. GaAs [46]. In our experiment, the TPA was roughly equal for both SESAM samples, while saturable losses differed by approximately a factor of two. Correspondingly, the balancing of the SAM by the TPA occurred at higher intensity in the high-absorbing sample, thus allowing higher pulse energy and shorter pulse duration (60–70 fs vs. > 100 fs with a low-absorbing sample).

We can conclude that in spite of the stronger tendency to multi-pulsing and high insertion losses of a SESAM in comparison to the pure KLM the use of the semiconductor saturable absorber may be attractive in case of a directly diode-pumped $\text{Cr}^{4+}:\text{YAG}$ laser [7] due to the lower mode-locking threshold. The multi-pulsing can be reduced by proper SESAM design.

4 Numerical modeling

In order to estimate the limits and ways to improve the stable self-starting operation at the highest achievable average and peak output power and mode-locking quality, i.e.

a chirp-free pulse envelope with smooth spectrum and minimum CW contribution, we performed a numerical modeling of our setup. Such analysis requires a multi-parametric optimization based on the numerical simulation of the KLM. A number of approaches to KLM modeling exists (for a review, see [47]), which can be divided into two general classes: (i) 2 + 1-dimensional simulation taking into account the details of the spatial field evolution and thereby considering the exact configuration of the laser and (ii) 1 + 1-dimensional simulation based on the generalized Landau–Ginzburg nonlinear equation considering KLM as a result of the effective fast saturable absorber action. We choose the latter approach as it is quite general and physically meaningful.

The basic model, which we use in this work, was described in [41] and proved its validity for the KLM Cr:LiSGaF laser. It takes into account such lasing factors as the relaxing gain saturated by the full ultra-short-pulse energy (for our Cr:YAG system the maximum unsaturated gain coefficient is 0.28 in double pass, the active crystal double length is $z = 4$ cm, the relaxation time is 4 μs , and the absorption and emission cross sections are $7 \times 10^{-18} \text{ cm}^2$ and $3.3 \times 10^{-19} \text{ cm}^2$, respectively); the linear loss involving the intracavity loss (2%) and the output loss with the coefficient $\rho = 1.5\%$ and 0.5%; the spectral filtering with the band coinciding with the gain band (inverse bandwidth $t_f = 5.4$ fs); the second-order group-delay dispersion with the coefficient $D = d\varphi/d\omega^2|_{\omega=\omega_0}$ ($\varphi(\omega)$ is the linear phase retardation of the field, ω is the frequency, $\omega_0 = 1.26$ PHz corresponds to the maximum of the gain band); the self-phase modulation defined by the nonlinear refraction coefficient $n_2 = 5.7 \times 10^{-16} \text{ cm}^2/\text{W}$; and, finally, the Kerr-lens fast saturable absorber with the modulation depth 2% and the inverse saturation intensity σ . It is convenient to normalize the σ parameter to the self-phase-modulation coefficient $2\pi n_2 z / \lambda n$ ($\lambda = 1.5 \mu\text{m}$ is the central oscillation wavelength, $n = 1.82$ is the linear refraction coefficient), making it dimensionless.

The saturation parameter σ is governed by the laser cavity alignment: the approach to the edge of the laser cavity stability zone increases σ [47]. The σ values can be estimated from the comparison of the experimental KLM output powers with those obtained from the quasi-soliton model [48]. In our case this results in $\sigma = 1.5 - 2.5$.

In the modeling, we consider the pump power P , the GDD parameter D , and σ to be the main parameters that are controlled in the experiment. The output loss ρ and the spectral bandwidth $1/t_f$ can be varied by the choice of the output mirror.

The simulations demonstrate a strong dependence of the ultra-short-pulse stability on these parameters. Figure 10 shows the pulse-stability regions on the D – σ plane and represents the typical optimization procedure due to the change of the prism separation (or their insertion into the laser beam) and the cavity realignment. For the fixed GDD, there is a minimum value of the saturation parameter required for the transition from the CW operation to the stable KLM. Its value can be estimated in the framework of the soliton model (dotted curves, see [49]). For fixed D , the higher saturation parameter corresponds to shorter pulses, but the pulse shortening eventually stops due to the transition to multi-pulsing at some higher σ value. The pulse-stability region is confined on σ [50]. Ad-

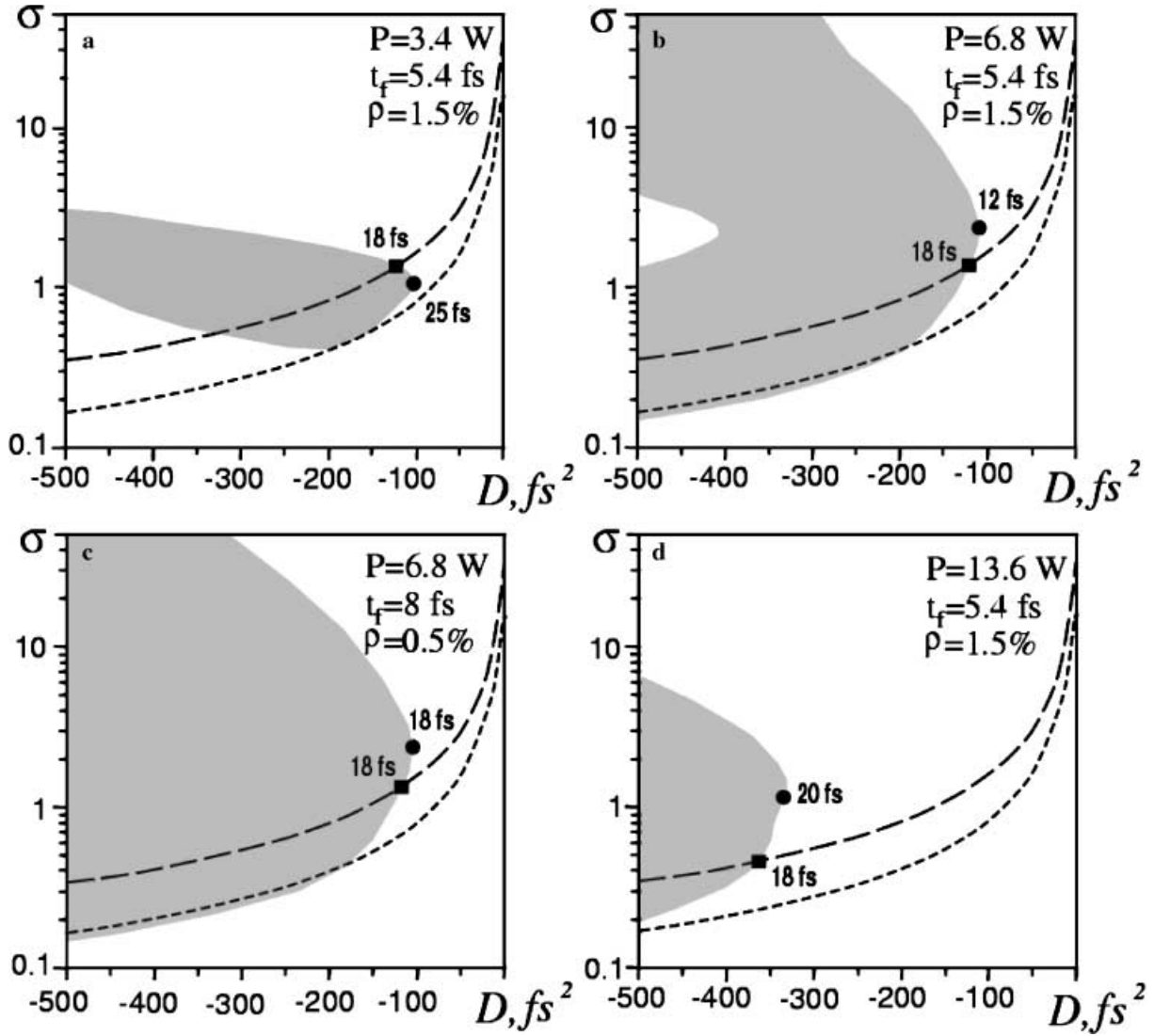


FIGURE 10 Regions of the stable single-pulse generation (gray); the parameters of the chirp-free pulses (dashed curves) and the pulse-stability threshold (dotted curves) from the soliton model; the parameters of the shortest chirp-free soliton-like pulses (squares) and the numerically simulated pulses (circles) with the duration shown by captions. a: $P = 3.4$ W, $t_f = 5.4$ fs, $\rho = 1.5\%$; b: $P = 6.8$ W, $t_f = 5.4$ fs, $\rho = 1.5\%$; c: $P = 6.8$ W, $t_f = 8$ fs, $\rho = 0.5\%$; d: $P = 13.6$ W, $t_f = 5.4$ fs, $\rho = 1.5\%$

ditionally, the pulse loses its stability in the vicinity of the zero GDD due to the transition to the regular or irregular multi-pulsing. As the minimal pulse durations correspond to $|D| \rightarrow 0$, this destabilization prevents the pulse shortening. Hence the main goals are the extension of the pulse-stability region on D and σ . The approach of the stability-region edge to zero GDD allows the shorter pulses and the extension of σ provides the KLM without thorough cavity optimization.

The described goals can be achieved by the variation of P . One can see that the pulse-stability zone for the pump power $P = 3.4$ W (Fig. 10a), which is close to the minimal pump level required for the KLM of our laser, is narrow, requiring very fine cavity alignment. Moreover, the relatively low intracavity pulse power is not sufficient for the pulse to become shorter than 25 fs (the parameters corresponding to the numerically estimated minimal pulse duration are marked by the circles in Fig. 10). For comparison, dashed curves show the parameters corresponding to the chirp-free pulses, obtained on the basis of the soliton model [48]. The minimal pulse du-

ration ≈ 18 fs, which is predicted by the soliton model (the square in Fig. 10), is too low an estimate for this pump level.

At a higher pump power of 6.8-W the zone of stable single-pulse KLM becomes broader (Fig. 10b). This favors the optimization procedure and shortens the numerically predicted pulse duration down to 12 fs. However, the comparison with the soliton model suggests that the shortest pulse is chirped and the shortest chirp-free pulse duration is about 18 fs. Further pump increase (Fig. 10d) leads to stronger multi-pulsing, narrowing the pulse-stability region. The minimum pulse duration gets longer and the pulse acquires a growing chirp. The pulse duration obtained from the soliton model is underestimated in this case, too.

Hence, there is an optimal pump level (which is close to 7 W in our particular case) that allows generation of the chirp-free pulses with the minimum duration ≈ 18 fs. The stability region is the widest for this pump level. The tendency to multi-pulsing can be suppressed by the t_f increase (Fig. 10c). In order to prevent the pulse broadening, the in-

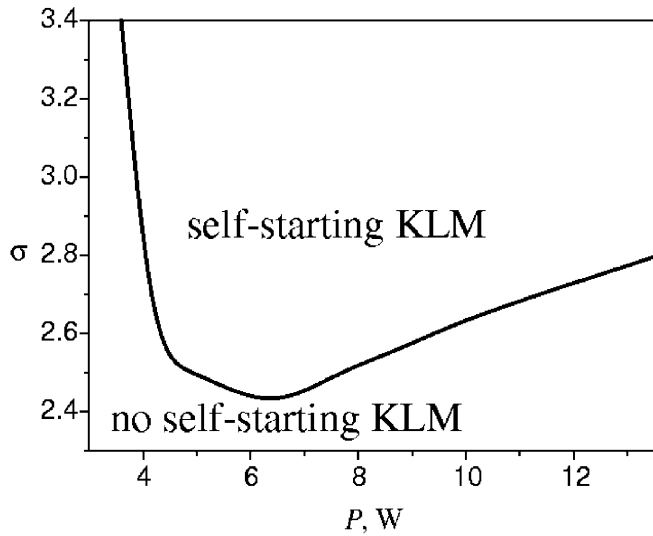


FIGURE 11 Self-starting KLM threshold for $q = 1.5\%$ (for other parameters, see text)

tracavity power has to be increased by lowering the output loss. This allows the 18-fs pulse generation with the maximum stability.

The crucial characteristic of KLM is not only the pulse stability but also the KLM self-starting ability. To investigate the latter we used the simpler model, which considers the mode-locking self-starting as the destabilization of the CW due to the auto-oscillations with angular frequencies $2\pi m/T_{\text{cav}}$ (T_{cav} is the cavity period, m is an integer) [51]. The corresponding minimal saturation parameters are shown in Fig. 11 in dependence on the pump rate. One can see that the pump powers below 3.5 W do not provide KLM self-starting. The minimum σ , which provides the self-starting KLM, corresponds to the optimal pump level ~ 7 W and is close to the experimentally observed value.

5 Conclusion

Summarizing, we demonstrated the first self-starting KLM Cr:YAG laser, pumped by a compact diode-pumped Yb-fiber laser and generating stable high-quality optical pulses at down to 26-fs pulse duration and at 250–450 mW of output power, and ~ 55 -fs pulses at the so far highest reported output power of 600 mW, without use of nitrogen purging of the cavity. The theoretical analysis yields the self-starting conditions and stability limits of existence of such transform-limited pulses. It also predicts the shortest achievable pulse durations at the given set of experimental parameters and provides an explanation of the spectral shift of the pulses observed in several experimental reports. Our experimental pulses are close to the shortest stable self-starting transform-limited pulses, which are theoretically achievable at the given experimental parameters. Even shorter pulses are possible, however, provided that the third- and the higher-order dispersions are taken into account and a significantly different set of experimental cavity parameters is chosen.

ACKNOWLEDGEMENTS It is our pleasure to thank Dr. A.V. Shestakov, E.L.S. Polyus, for supplying the Cr:YAG crystals, and

Dr. John Alcock and Dr. Philip Poole, NRC Institute for Microstructural Sciences, for providing the SESAM samples. This work has been performed under Austrian Fonds zur Förderung der Wissenschaftlichen Forschung Grant Nos. T64, M611, and P14704-TPH, and BMBWK Grant No. B631.

NOTE ADDED IN PROOF Recently we were able to obtain self-starting passive mode-locking of the directly diode-pumped Cr⁴⁺:YAG laser using a SESAM, and obtaining 50-fs transform-limited pulses with 15 mW average output power.

REFERENCES

- N.B. Angert, N.I. Borodin, V.M. Garmash, V.A. Zhitnyuk, A.G. Okhrimchuk, O.G. Siyuchenko, A.V. Shestakov: *Sov. J. Quantum Electron.* **18**, 73 (1988)
- N.I. Borodin, V.A. Zhitnyuk, A.G. Okhrimchuk, A.V. Shestakov: *Bull. Acad. Sci. USSR Phys. Ser.* **54**, 54 (1990)
- H. Eilers, W.M. Dennis, W.M. Yen, S. Kueck, K. Petermann, G. Huber, W. Jia: *IEEE J. Quantum Electron.* **QE-29**, 2508 (1993)
- A.G. Okhrimchuk, A.V. Shestakov: *Opt. Mater.* **3**, 1 (1994)
- C.R. Pollock, D.B. Barber, J.L. Mass, S. Markgraf: *IEEE J. Sel. Top. Quantum Electron.* **1**, 62 (1995)
- I.T. Sorokina, S. Naumov, E. Sorokin, E. Wintner: *Advanced Solid-State Lasers*, ed. by M.M. Fejer, H. Injeyan, U. Keller (OSA Trends Opt. Photon. **26**) (Optical Society of America, Washington, DC 1999) pp. 331–335
- I.T. Sorokina, S. Naumov, E. Sorokin, E. Wintner: *Opt. Lett.* **24**, 1578 (1999)
- S. Naumov, E. Sorokin, I.T. Sorokina: 'Actively Mode-locked Directly Diode-pumped CW Room-temperature Cr⁴⁺:YAG Laser'. In: *Tech. Dig. Conf. Lasers Electro-Opt. (CLEO 2001)*, Postconf. edn. (OSA Trends Opt. Photon. **56**) (Optical Society of America, Washington, DC 2001) pp. 340–341
- P.M.W. French, N.H. Rizvi, J.R. Taylor, A.V. Shestakov: *Opt. Lett.* **18**, 39 (1993)
- A. Sennaroglu, C.R. Pollock, H. Nathel: *Opt. Lett.* **19**, 390 (1994)
- P.J. Conlon, J.P. Tong, P.M. French, J.R. Taylor, A.V. Shestakov: *Opt. Lett.* **19**, 1468 (1994)
- P.J. Conlon, J.P. Tong, P.M. French, J.R. Taylor, A.V. Shestakov: *J. Mod. Opt.* **42**, 723 (1995)
- J. Ishida, K. Naganuma: *Opt. Lett.* **21**, 51 (1996)
- B.C. Collings, J.B. Stark, S. Tsuda, W.H. Knox, J.E. Cunningham, W.Y. Jan, R. Pathak, K. Bergmann: *Opt. Lett.* **21**, 1171 (1996)
- Y.P. Tong, P.M.W. French, J.R. Taylor, J.O. Fujimoto: *Opt. Commun.* **136**, 235 (1997)
- S. Naumov, E. Sorokin, I.T. Sorokina: 'Tunable Diode-pumped CW Mode-locked Cr⁴⁺:YAG Laser'. In: *Conf. Dig. CLEO/Europe-EQEC Focus Meet.* (European Physical Society, Mulhouse 2001) p. 33
- Y.P. Tong, L.M. Sutherland, P.M.W. French, J.R. Taylor, A.V. Shestakov, B.H.T. Chai: *Opt. Lett.* **21**, 644 (1996)
- Y. Ishida, K. Naganuma: *Opt. Lett.* **19**, 2003 (1994)
- J. Theimer, M. Hayduk, M.F. Krol, J.W. Haus: *Opt. Commun.* **142**, 55 (1997)
- S. Spaelter, M. Boehm, M. Burk, B. Mikulla, R. Fluck, I.D. Jung, G. Zhang, U. Keller, A. Sizmman, G. Leuchs: *Appl. Phys. B* **65**, 335 (1997)
- M.J. Hayduk, S.T. Johns, M.F. Krol, C.R. Pollock, R.P. Leavitt: *Opt. Commun.* **137**, 55 (1997)
- Z. Zhang, T. Nakagawa, K. Torizuka, T. Sugaya, K. Kobayashi: *Opt. Lett.* **24**, 1768 (1999)
- Z. Zhang, T. Nakagawa, K. Torizuka, T. Sugaya, K. Kobayashi: *Appl. Phys. B* **70** [Suppl.], S59 (2000)
- B.C. Collings, K. Bergman, W.H. Knox: *Opt. Lett.* **22**, 1098 (1997)
- R. Mellish, S.V. Chernikov, P.M. French, J.R. Taylor: *Electron. Lett.* **34**, 552 (1998)
- T. Tomaru, H. Petek: *Opt. Lett.* **25**, 584 (2000)
- T. Tomaru: *Opt. Lett.* **26**, 1439 (2001)
- H.A. Haus, J.D. Moores, L.E. Nelson: *Opt. Lett.* **18**, 51 (1993)
- T. Tomaru, H. Petek: *J. Opt. Soc. Am. B* **18**, 388 (2001)
- S.M.J. Kelly: *Electron. Lett.* **28**, 806 (1992)
- Q. Lin, I. Sorokina: *Opt. Commun.* **153**, 285 (1998)
- D.J. Ripin, C. Chudoba, J.T. Gopinath, J.G. Fujimoto, E.P. Ippen, U. Morgner, F.X. Kärtner, V. Scheuer, G. Angelow, T. Tschudi: *Opt. Lett.* **27**, 61 (2002)

- 33 F.X. Kärtner, N. Matuschek, T. Schibli, U. Keller, H.A. Haus, C. Heine, R. Morf, V. Scheuer, M. Tilsch, T. Tschudi: *Opt. Lett.* **22**, 831 (1997)
- 34 R. Szipöcs, K. Ferencz, Ch. Spielmann, F. Krausz: *Opt. Lett.* **19**, 201 (1994)
- 35 R. Szipöcs, A. Kohazy-Kis: *Appl. Phys. B* **65**, 115 (1997)
- 36 G. Tempea, F. Krausz, Ch. Spielmann, K. Ferencz: *IEEE J. Sel. Top. Quantum Electron.* **4**, 193 (1998)
- 37 A.J. Alcock, P.J. Poole, B.T. Sullivan: 'Hybrid Semiconductor Saturable Absorber Mirrors as Passive Mode-locking Elements'. In: *OPTO Can., SPIE Reg. Meet. Optoelectron. Photon. Imaging, Ottawa, 9–10 May 2002*, paper CA01-506
- 38 G. Cerullo, S. De Silvestri, V. Magni, L. Pallaro: *Opt. Lett.* **19**, 807 (1994)
- 39 M. Piche, F. Salin: *Opt. Lett.* **18**, 1041 (1991)
- 40 H.A. Haus, I. Sorokina, E. Sorokin: *J. Opt. Soc. Am. B* **15**, 223 (1998)
- 41 V.L. Kalashnikov, E. Sorokin, I.T. Sorokina: *J. Opt. Soc. Am. B* **18**, 1732 (2001)
- 42 I.T. Sorokina, E. Sorokin, E. Wintner, A. Cassanho, H.P. Jenssen, R. Szipöcs: *Opt. Lett.* **21**, 1165 (1996)
- 43 I.T. Sorokina, E. Sorokin, E. Wintner, A. Cassanho, H.P. Jenssen, R. Szipöcs: *Opt. Lett.* **22**, 1716 (1997)
- 44 S. Namiki, E.P. Ippen, H.A. Haus, C.X. Yu: *J. Opt. Soc. Am. B* **14**, 2099 (2001)
- 45 E.R. Thoen, E.M. Koontz, M. Joschko, P. Langlois, T.R. Schibli, F.X. Kärtner, E.P. Ippen, L.A. Kolodziejski: *Appl. Phys. Lett.* **74**, 3927 (1999)
- 46 M.D. Dvorak, B.L. Justus: *Opt. Commun.* **114**, 147 (1995)
- 47 V.P. Kalosha, M. Müller, J. Herrmann, S. Gatz: *J. Opt. Soc. Am. B* **15**, 535 (1998)
- 48 H.A. Haus, J.G. Fujimoto, E.P. Ippen: *IEEE J. Quantum Electron.* **QE-28**, 2086 (1992)
- 49 A.K. Komarov, K.P. Komarov: *Opt. Commun.* **183**, 265 (2000)
- 50 V.L. Kalashnikov, E. Sorokin, I.T. Sorokina: 'Multipulse Operation and Limits of the Kerr-lens Mode Locking Stability for Cr²⁺:ZnSe Laser'. In: *Tech. Dig. Advanced Solid-State Lasers (OSA Trends Opt. Photon. 68)* (Optical Society of America, Washington, DC 2002) p. WA8-1-3
- 51 V.L. Kalashnikov, D.O. Krimer, I.G. Poloyko, V.P. Mikhailov: *Proc. SPIE* **3683**, 225 (1998)